J Ther Eng, Vol. 9, No. 6, pp. 1632−1642, November, 2023

Journal of Thermal Engineering
Web page info: https://jten.yildiz.edu.tr
DOI: 10.18186/thermal.1401534

Journal of Thermal Engineering

Research Article

Experimental study on heat transfer from rectangular fins in combined convection

Mehdi BASIRI[2], Hamid Reza GOSHAYESHI[2,*], Issa CHAER[3], Hadi POURPASHA[4], Saeed Zeinali HERIS[1,*]

[1]Xi'an University of Science and Technology, No.58, Middle Section of Yanta Road, Xi'an, Shaanxi, China 710054
[2]Department of Mechanical Engineering, Azad University, Mashhad Branch, Mashhad, Iran
[3]Centre for Civil and Building Services Engineering, School of the Built Environment and Architecture, London South Bank University, London, SE1 0AA UK
[4]Faculty of Chemical and Petroleum Engineering, University of Tabriz, Tabriz, Iran

ARTICLE INFO

Article history
Received: 12 June 2022
Accepted: 17 December 2022

Keywords:
Plate Heat Sink; Combined Convection; Rectangular Fin; Richardson Number; Empirical Equation

ABSTRACT

Combined natural and forced convective heat transfer arise in many transport processes in engineering devices and in nature, which is frequently encountered in industrial and technical processes, including electronic devices cooled by fans, heat exchangers placed in a low-velocity environment, and solar receivers exposed to winds. In this study, the effects of design parameters have been experimentally investigated for the air-side thermal performance under combined (natural and forced) convection of the rectangular plate heat sinks, and the values of optimum design parameters were sought. Many ideas for improving cooling methods have been proposed, one of which is the heat sink. In this work, the average Nusselt number (Nu) and thermal resistance of a simple base rectangular plate and five vertical rectangular plate heat sinks with different numbers of fins under natural and combined convection were experimentally investigated to obtain the maximum average Nu and minimum thermal resistance for various Reynolds numbers (Re) from 2300 to 40000, Rayleigh numbers (Ra) from 1300000 to 13000000, and Richardson numbers (Ri) from 0.4 to 3. Also, in this experiment, fin spacing (P) was varied from 2.8 mm to 14.6 mm and the dimensionless P/H ratio was varied from 0.1 to 0.49. The flow velocity varied in the range of 2 to 8 m/s under combined convection. Based on the effects of Ri and Re, two empirical equations for natural and also for combined convection heat transfer were derived to calculate the average Nu. The average deviation for these two equations is about 7%. The outcomes of this research can be beneficial for engineers who work on electronics cooling systems.

Cite this article as: Basiri M, Goshayeshi HR, Chaer I, Pourpasha H, Heris SZ. Experimental study on heat transfer from rectangular fins in combined convection. J Ther Eng 2023;9(6):1632−1642.

***Corresponding author.**
*E-mail address: SZ.Heris@xust.edu.cn

This paper was recommended for publication in revised form by Regional Editor Jaap Hoffman Hoffman

INTRODUCTION

Due to the rapid development of technology, electronic devices are a part of our ordinary lives. There are various methods to cool electronics, such as air flow cooling and heat pipe. Air flow with heat sink was used in conventional electronics cooling systems, which would show superiority in terms of unit price, weight, and reliability. Therefore, the most common way to enhance the air-cooling is through the utilization of air flow on a heat sink. Considering the large amount of heat produced by chemical and industrial companies (power plants, refineries, petrochemical companies), improving the heat transfer performance of equipment is desired. There are many studies in the literature on heat transfer enhancement using different techniques [1, 2]. One of the most commonly used techniques for heat transfer enhancement is fins [3]. The extensive use of finned surfaces to improve heat transfer in engineering equipment such as heat exchangers, cooling towers, and chemical reactors makes it critical to study methods to increase heat transfer from the fins [4-6]. For the cooling of computer processors and other electronic instruments, fins are used to enhance the rate of heat transfer. According to the available literature, an immense number of experimental studies of combined convection heat transfer from finned surfaces have been conducted. Kobus et al. [7] carried out an analytical study to find the effect of buoyancy on laminar combined convection in a staggered vertical pin fin array. Kobus and Oshio [8] developed a theoretical model for a vertical pin-fin array heat sink for combined convection. Haghighi et al. [9] investigated the impact of a novel design of plate-fin-based heat sinks on convection heat transfer. Their results indicated that heat transfer improved by about 10%–41.6%. Yang et al. [10] investigated heat transfer in an angled parallel-plate channel with a transverse fin situated at the channel's lower wall. They reported that the optimum aspect ratio of a fin corresponding to a fin with the maximum heat transfer rate improves with raising Re. For a mixed convection flow in a parallel-plate channel, the optimum aspect ratio of a fin reduces as the ratio of the fin's thermal conductivity to the fluid's thermal conductivity rises. Li and Chao [11] studied the different shapes of fins on a heated horizontal base plate. They proposed some correlations related to fin spacing, fin height, and ambient temperature.

Numerous experimental and numerical studies concerning the rectangular fin arrays have been conducted. The influence of the transverse pitch and the longitudinal pitch of the tube bundles, the transverse fin spacing, and the height of the fin on the heat transfer and resistance characteristics of the pin-fin tube bundle was investigated by Wang et al. [12]. Based on the available literature, the following recent studies show the main parameters affecting the convection behavior or fin arrays such as fin shape and thickness [13-15], surface area [16], material [17, 18], vertical fin arrays [19-21], horizontal arrays [22], air velocity [23, 24], spacing of the fin [25, 26], and fin angle [27, 28]. Yeom et al. [13] investigated the effects of fin height and fin spacing on combined convection heat transfer from rectangular fin. They reported that the optimal value of fin spacing is mostly determined by modified Ra. The thermal performance and mechanics of a double-layer microchannel heat sink were investigated by Xu et al. [14]. Their findings showed that cutting the baffle of micro-channels enhances heat transmission and thermal stress performance significantly. Gaikwad et al. [16] numerically investigated the pool boiling heat transfer on isothermal elliptical tubes with various aspect ratios in saturated conditions. Their results indicated that with decreasing the aspect ratio, the first bubble tip velocity and departure time increase and decline, respectively. Muhammed et al. [18] investigated the impact of a V-type fin on heat transfer performance from a vertical surface. Their findings demonstrated that the V-shaped fin performs better because it allows air to move quicker through the center channel that separates the fin array. Shim et al. [21] examined the heat transfer effects of slanted-pin fins on an inclined hot surface. In a vertical channel, with rising buoyancy-driven flow, the heat performance of the positively inclined fins was better than the negatively inclined fins. Other studies include flow regime (laminar, transitional, turbulence) [29, 30], natural and forced phase convection [31, 32], use of PCM in heat sinks [33, 34], and use of ribs in heat sinks [35]. Li et al. [36] studied the thermal performance of plate-fin sinks. Their findings suggest that the thermal performance increases with an increasing Re up to a point when the improvement becomes limited. Singh et al. [37] investigated the enhancement of heat transfer through an embossed fin heat sink under natural convection. They discovered that an impression angle of 45° and an impression pitch of 12 mm produce the best results.

The above studies show the necessity of studying and optimizing the plate heat sink on the vertical base plate. Although the traditional plate heat sink has been previously researched, there was no complete practical model to predict the Nu for combined convection.

The purpose of the current work is to measure the average convective Nu and the thermal resistance of the heat sink by using an experiential measurement technique. The experimental investigation for the plate heat sink will provide design insight, including the existence of optimum fin spacing. In this paper, six heat sinks with different rectangular fin arrays under combined convective heat transfer were investigated and found the optimum arrangement.

Theory of Combined Convection

Many processes in engineering devices and nature [38] involve combined convective heat transfer, which is frequently encountered in industrial and technical processes such as electronic devices cooled by fans, nuclear reactors cooled during emergency shutdown, heat exchangers

placed in a low-velocity environment, and solar receivers exposed to winds.

In dealing with forced convection, we ignored the effects of natural convection. This was, of course, an assumption, for, as we now know, natural convection is likely when there is an unstable temperature gradient. Similarly, in the preceding sections of this part, we assumed that forced convection was negligible. It is now time to acknowledge that situations may arise for which natural and forced convection effects are comparable, in which case it is inappropriate to neglect either process.

For the specific geometry of interest, the Nu, Nu_F and Nu_N are determined from existing correlations for pure forced and natural (free) convection, respectively.

$$Nu_{ave} = Nu_F^n \mp Nu_N^n \quad (1)$$

The plus sign on the right-hand side of Equation (1) applies to assisting and transverse flows, while the minus sign applies to opposing flows [39]. The best correlation of data is often obtained for n=3.5 for cross flows.

The convection heat transfer regime is determined using Ri ($Ri = \frac{Gr}{Re^2} = \frac{Ra}{Pr\,Re^2}$). This dimensionless group can be expressed in terms of the physical parameter as if [39]:

$Ri = \frac{Ra}{Pr\,Re^2} \simeq 1$ Combined convection

$Ri = \frac{Ra}{Pr\,Re^2} \ll 1$ Forced convection

$Ri = \frac{Ra}{Pr\,Re^2} \gg 1$ Natural convection dominates

Re calculated by using the equation (1) [11]:

$$Re = \frac{\rho U D_h}{\mu} \quad (2)$$

where U is the inlet velocity of the cooling air; D_h ($D_h = \frac{4A_c}{P}$) is the hydraulic diameter of the test section, μ is the dynamic viscosity of air, Gr is the Grashof number, and Pr is the Prandtl number.

Experimental Apparatus

The set-up consists of various instruments for measuring the ambient temperature; the rear surface of the heater temperature; the temperature of the front surface of the heater; the temperature of the air (as close as possible to the fin configuration); and the input power of the heater. Special attention was paid to the insulation of the rear surface of the heater.

For choosing a suitable insulation, we know that only the thickness (L) and the thermal conductivity (k) of the insulation are important for the conduction of heat through it. Hence, the heat loss through the plate can be eliminated by letting either L→∞ or k→0. Since a plate of L→∞ or k→0 is physically impossible, the foregoing insulation may never be accomplished in the absolute sense. However, the larger the thickness or the smaller the thermal conductivity, the better the insulation will be.

The temperature of the surfaces of the epoxy plate that are in contact with the heater is adjusted to the same degree, which almost eliminates the heat loss from the rear surface of the heater. The lateral surface of the heater is insulated by rock wool.

The electrical power was supplied through a regulated AC power supply. The input power of the heater could be selected precisely by feeding the power to a variable transformer (Variac). The voltage drop and the current flow were monitored by a voltmeter-ammeter combination; the supplied power is calculated by multiplying the voltage drop and the current through the heater [40].

Figure 1(a) shows the schematic experimental setup, including the heater, guard heater, and Variac. The Dirichlet boundary condition is considered by using a thermo foil for the back of the heater and is carefully insulated using a guard heater. Epoxy and hardener were used to fill the gap between the heater and the guard heater and for insulation purposes, rock wool was used. A Variac was used to select the right amount of power, and by using a voltmeter-ammeter, the voltage drop and the current flow were monitored. The applied thermal power and heat flux can be calculated by using the equations (3), (4) [9]:

$$q = V \times I \quad (3)$$

$$q'' = q/A \quad (4)$$

where q is the heat input, V and I are the applied voltage and the intensity of the current, q" is heat flux and A is the area of our base plate, respectively. In Figure 1(b), the main heater, copper plate, and heat sink are presented. As can be seen in figure 3, a speed controller was used for controlling the fan speed. A digital voltmeter was also applied to measure the energy input of the DC fan. A hot-wire anemometer with an accuracy of 0.01 m/s was used to measure the flow velocity of the air. Fan speed, fin spacing, and heat input are the important factors for combined convection heat transfer. Fin spacing and heat input are the important factors for natural convection. In this experiment, to measure the baseplate and fin surface temperatures, thermocouples of type TM-946 were used. Figure 1(c) indicates the real photo of experimental setup

Figure 2 shows a rectangular base plate and five types of heat sinks used in the experimental study. The base plate meets the spreading resistance through the area difference between the base plate and the heat source. The heat sinks were made from the aluminum alloy 6061 (which has a thermal conductivity of 170 W/m K). The surface areas of the heaters were 48 mm*50 mm. Measuring instruments range and accuracy showed in Table 1.

From Eq. 5, voltage (V) and current (I) were the electrical parameters measured in our experiments, from

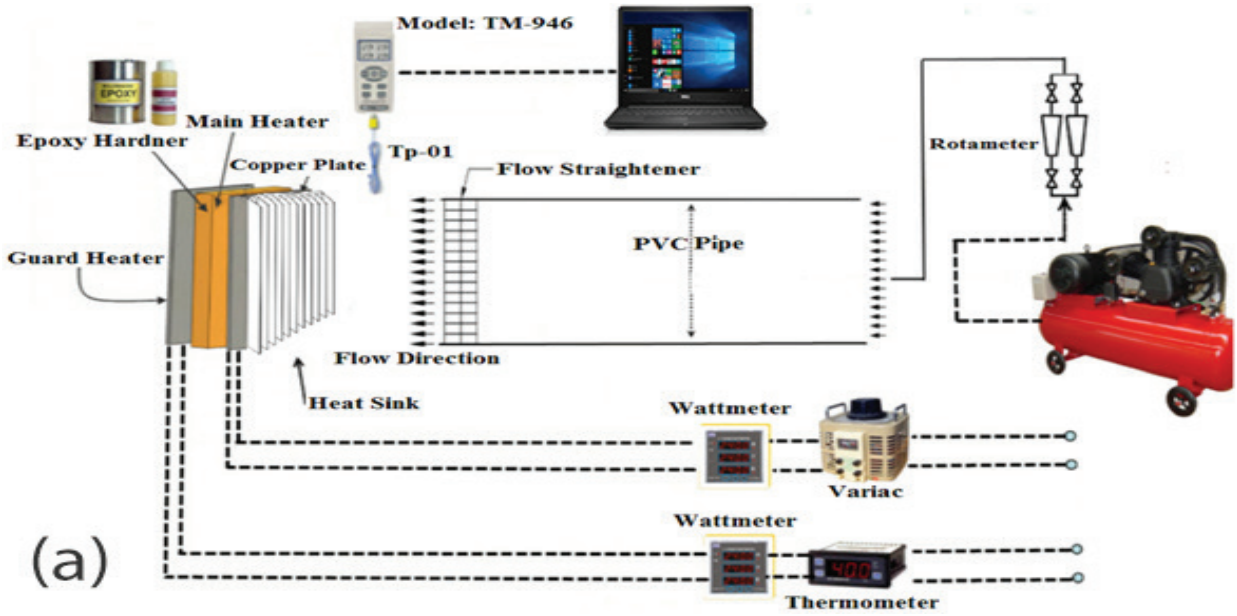

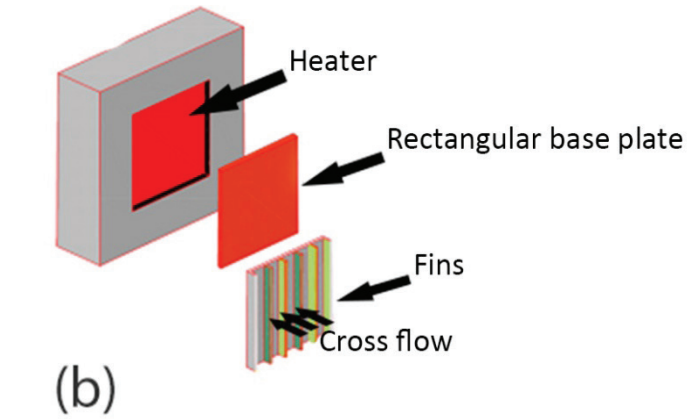

Figure 1. (a) Schematic of the experiment, (b) schematic view of our heat sink with heater, and (c) real photograph of setup.

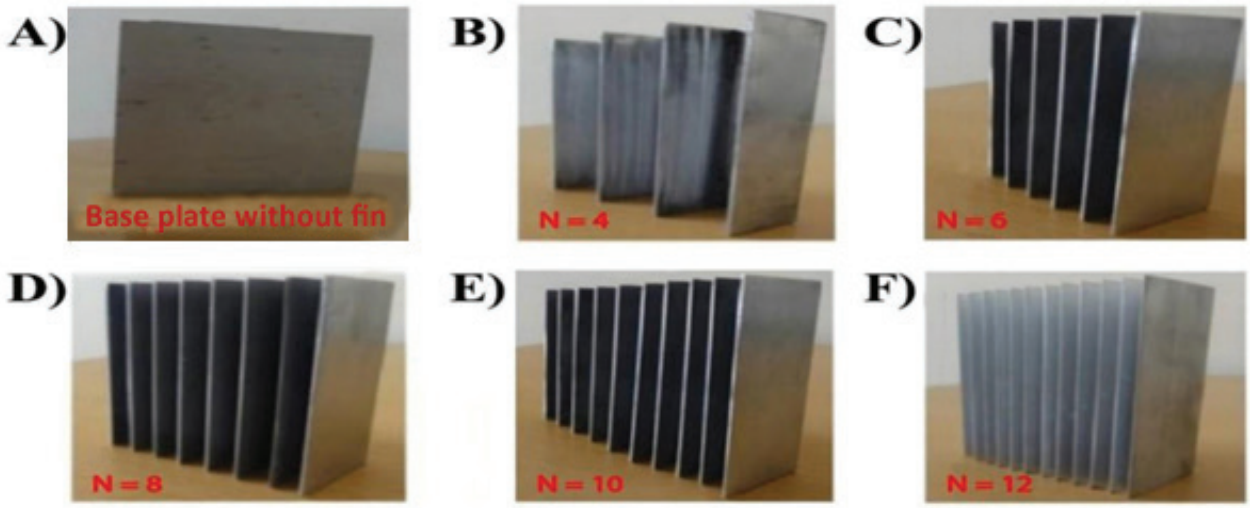

(a)

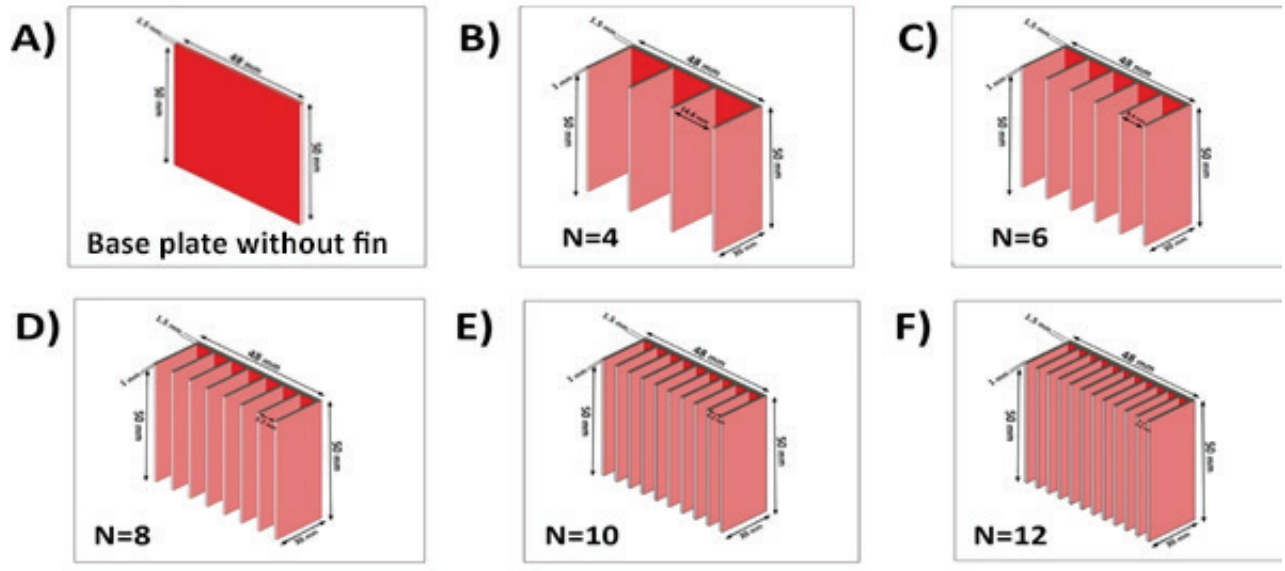

(b)

Figure 2. Heat sinks configurations: (a) Real photos and (b) Schematics.

Table 1. Instruments used

Parameter	Measurement device	Measurement Range	Accuracy
Ambient temperature	K type	0 to 300 °C	±0.1 C
Surface temperature	TM-946	0 to 300 °C	±0.1 C
Voltage measurement	Variac	0 to 300 V	±0.1 V
Current	Multimeter	0 to 20 A	±0.1 A
Length measurement	Caliper	5 m	±0.01 m

Table 2. Fins configuration used in this experiment

Fin shape	Fin spacing (S (mm))	Fin height (H(mm))	S/H	Fin number (N)
Plain plate A	-	-	-	-
Heat sink B	14.6	30	0.49	4
Heat sink C	8.4	30	0.28	6
Heat sink D	5.7	30	0.19	8
Heat sink E	4.2	30	0.14	10
Heat sink F	2.8	30	0.1	12

which the input heat can be calculated. The total accuracy of the measurements was evaluated based on the accuracy of the employed instruments in the previous sub-section. The maximum uncertainty for the measurements can be obtained using the uncertainty concept provided in [41].

To calculate the uncertainty of the experimental measurements, the following relation is used [41]:

$$\omega_R = \left[\sum \left(\frac{\partial R}{\partial x_i}\omega_i\right)^2\right]^{1/2} \quad (5)$$

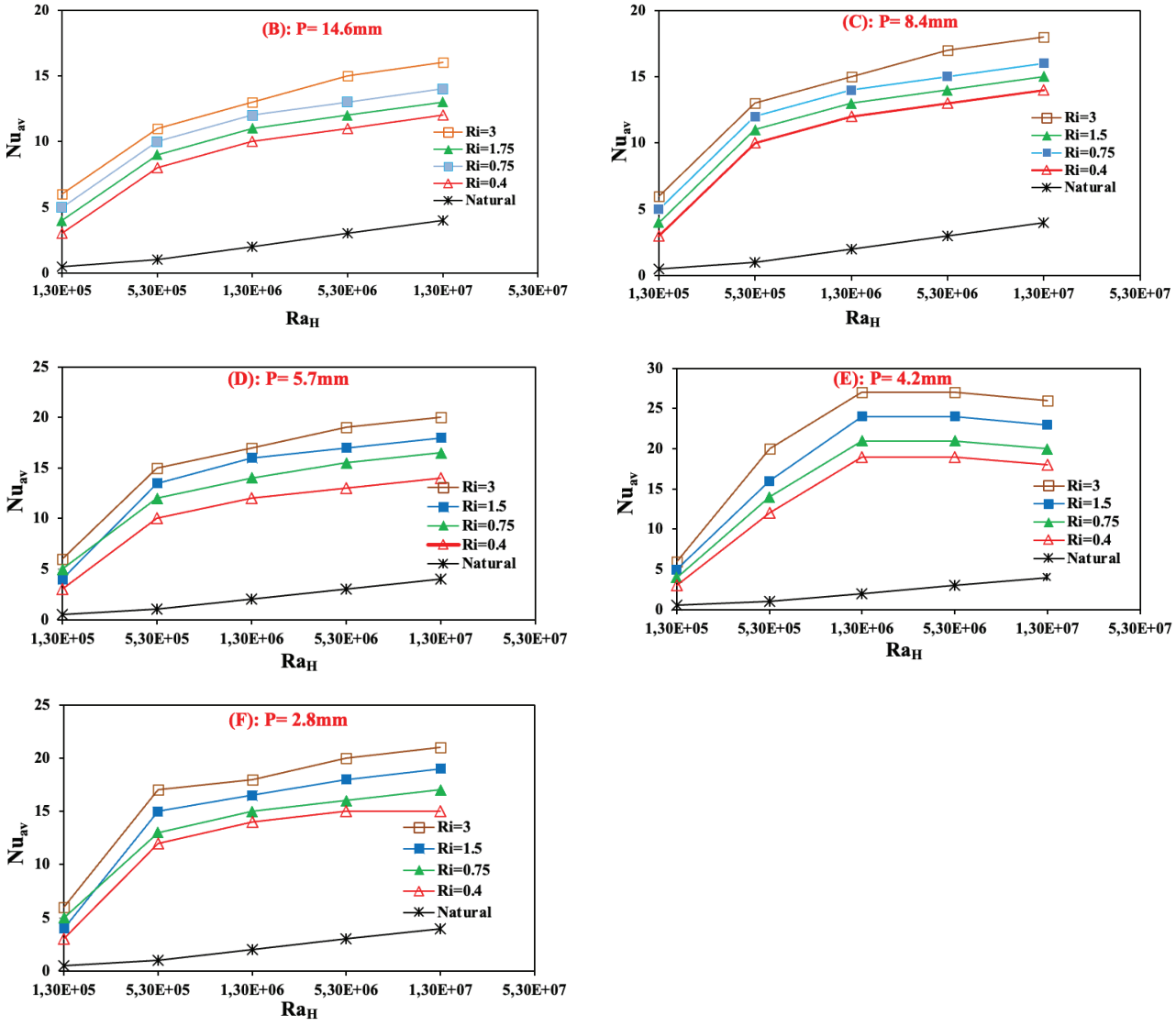

Figure 3. (B-F) Variation of Nu, Ra, and Ri for different fin spacing and under natural and combined convection at q" = 20833 W/m^2.

Where ω_R is the uncertainty in results, R($x_1, x_2, \ldots x_n$), and ω_i is the uncertainty of the independent variable x_1. According to Eq. 6;

$$\frac{\delta q}{q} = \sqrt{\left(\frac{\delta V}{V}\right)^2 + \left(\frac{\delta I}{I}\right)^2}, \quad (6)$$

The measured temperature uncertainties were reported as error bars in the experimental results. It should be noted that the error bars corresponding to the power measurement uncertainty are not visible due to their relatively small values as compared to the uncertainty values for the power.

In this experiment Ra changed from1 300000 to 13000000 and Re changed from 2 300 to 40 000, Ri varied from 0.4 to 3, and ratio of (P/H) varied from 0.1 to 0.49. Table 2 shows fins configuration used in this experiment.

RESULTS AND DISCUSSION

The combined convective heat transfer coefficient was investigated in this study under different Re and Ri and fin spacing. The investigation was conducted for Re varying from 2 300 to 40 000, Ra from 1300 000 to 13 000 000, and Ri from 0.4 to 3. Under combined convection, the flow velocity varied in the range of 2 to 8 m/s. The experimental results were obtained by changing the fin spacing from 14.6 mm to 2.8 mm and also the P/H ratio was varied from 0.1 to 0.49. For different values of fin spacing and Ri, the variations of Nu versus Ra are shown in Figure 3 (B-F). As it can be seen, the forced convection dominates as Nu values increase by 20%–40% when Ri changes from 0.4 to 3, respectively. Moreover, at specific values of Ri and fin spacing, Nu increased with an increase in Ra. The flow velocity of air from fin array has drastically increased Nu_{av} for P = 4.2 mm at Ri = 3.

Figure 4 (B-F) shows the effect of fin spacing on thermal resistance (R) for different Ri. It can be seen that as the fin spacing increases, thermal resistance ($R = \frac{\Delta T}{q}$) decreases to its minimum. The lowest thermal resistance is achieved for fin number type "E" with P = 4.2 mm and N = 10. Fig. 4(E) shows that the overall thermal resistance of the heat

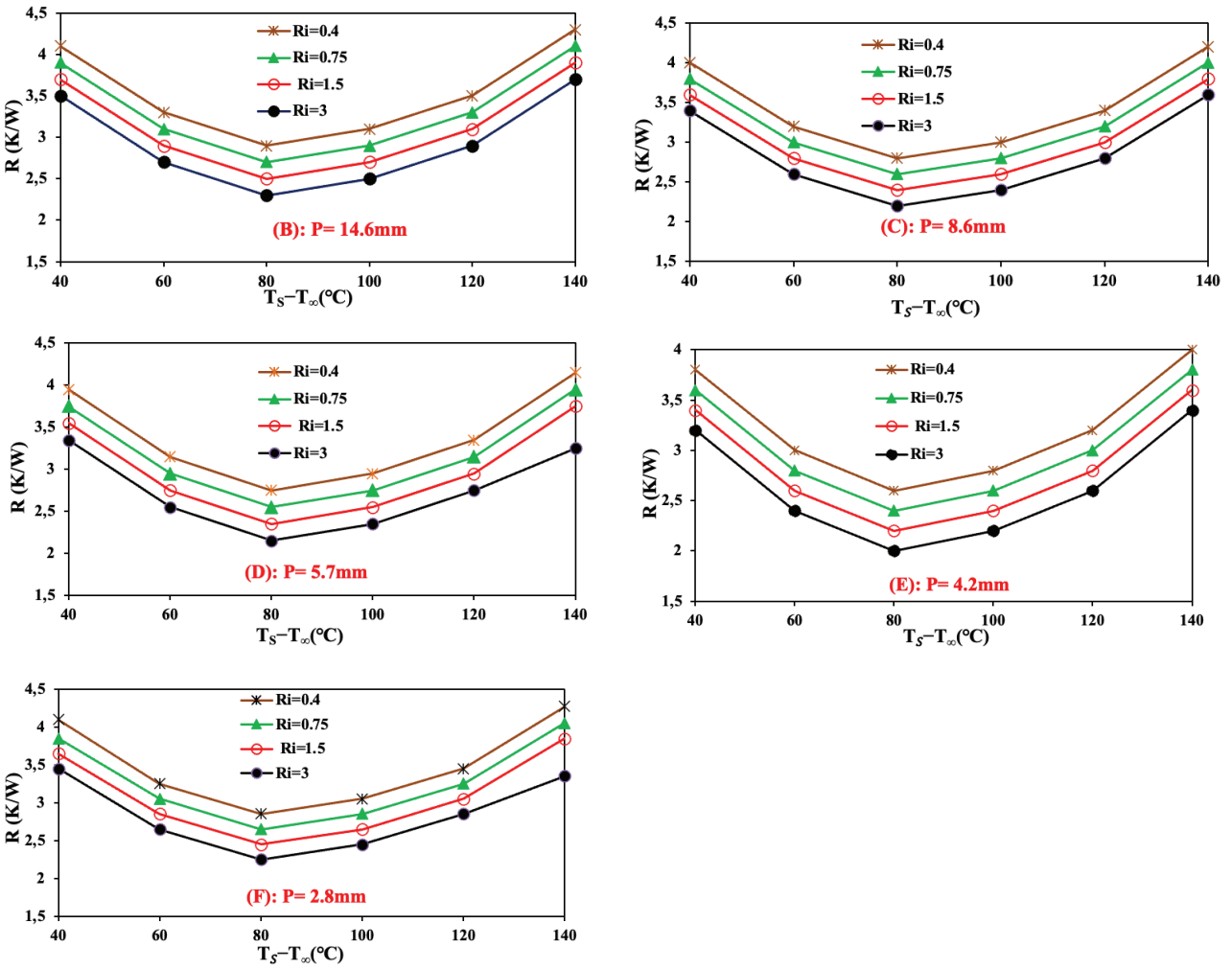

Figure 4. (B-F) Thermal resistance versus in spacing under combined convection for different Ri and heat input.

sink has a minimum value of about 2.25 C/W, with the fin spacing (pitch) at 4.2 mm. As the total height of the heat sink is fixed, convective resistances increase as the growth of the heat sink base causes the immersed heat transfer area to decrease and lowers air velocity. The value of fin spacing at which the heat transfer takes its maximum value is defined as the optimum fin spacing, P_{opt}. These figures show that the optimum fin spacing is 4.2 mm. The decrease in fin spacing causes an intersection between boundary layers developed on fin surfaces. The intersection of boundary layers, causing the velocity of fluid flowing through fin arrays to decrease, prevents the cold fluid from entering the fin grooves, and thus the hot fluid stays much longer between the fin arrays.

However, thermal resistance differences for different fin types are considerable at lower fin spacing. If fins are too close together, like type F at P=2.8 mm with N=12, boundary layers on adjoining surfaces will coalesce and heat transfer will decrease. If fins are too far apart, like type B at P=14.6 mm with N=4, the surface area becomes too small and thermal resistance decreases.

Like other researchers such as [40, 42], this study shows that the Nu is affected by some factors, such as Re, Gr, and fin height. By considering the effects of these parameters, an empirical equation was derived for Nu. Figure 5 shows the comparison of experimental results for combined heat transfer obtained from this work according to the effects of the mentioned parameters

The Gr, which is the ratio of the buoyancy force to the viscous force, can be defined as follows [40, 42]:

$$Gr = \frac{g\beta\Delta TH^3}{\vartheta^2} \quad (7)$$

Also, the Ra is defined as [1]:

$$Ra = Gr.Pr \quad (8)$$

$$Pr = \frac{Cp\mu}{k} \quad (9)$$

Natural convection for rectangular fin is assumed as a function of Ra, fin number, and ratio of P /H [43].

$$Nu = f(N, P/H, Ra) \quad (10)$$

According to experimental results, for the correlation of the average Nu for natural convection, the general form of the correlation function is given in equation (11). This equation is transformed by taking its logarithm to yield equation (12). The logarithm of the dependent variable is linearly dependent on the logarithms of the independent variables.

$$Nu = a\,N^b\,(P/H)^c\,Ra^d \quad (11)$$

$$\log Nu = \log a + b \log N + c \log (P/H) + d \log (Ra) \quad (12)$$

Also for correlating of the average Nu for combined convection [44], general form of the correlation function is given in equation (13):

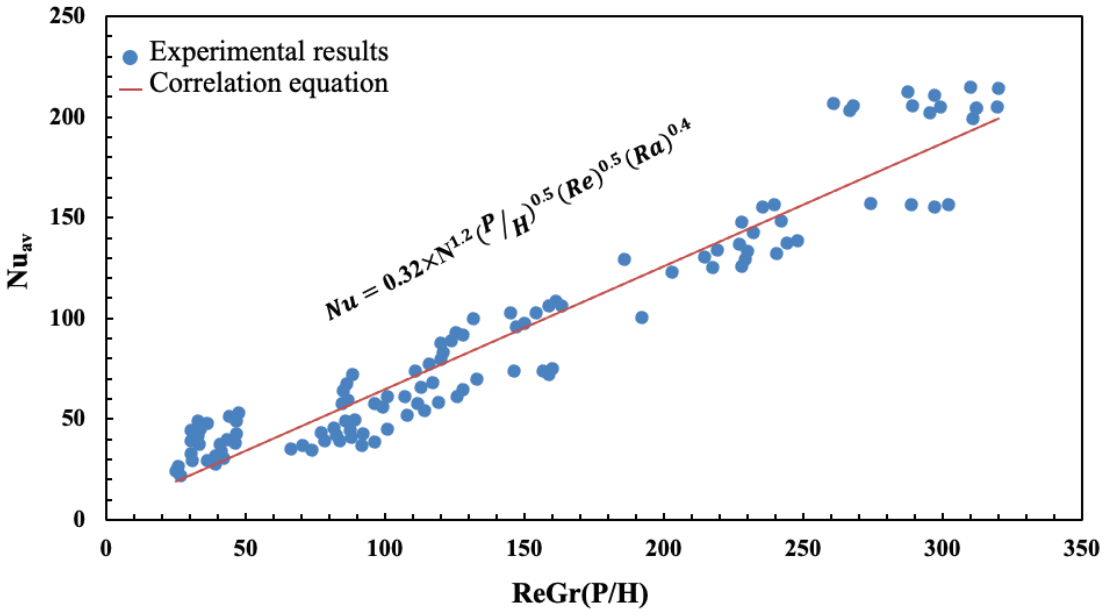

Figure 5. Comparison of experimental result for combined heat transfer obtained from this work.

$$Nu = aN^{b}(P/H)^{c}\,Re^{d}\,Ra^{e} \quad (13)$$

$$\text{Log Nu} = \log a + b \log N + c \log (P/H) + d \log Re + e \log Ra \quad (14)$$

According to experimental results, for correlating of the average Nu, two equations (Eqs. (15) and (16)) were developed as a function of Ra and Re, height ratio (P /H), and of number of plates (N). For obtaining an empirical equation for natural and combined convection least square regression method was applied [43]. Resulting equations are presented follows:

$$Nu = 0.107 \times N^{1.2} \left(\frac{P}{H}\right)^{0.5} (Ra)^{0.4} \quad (15)$$

(Natural convection correlation)

$$Nu = 0.32 \times N^{1.2} \left(\frac{P}{H}\right)^{0.5} (Re)^{0.5}\,(Ra)^{0.4} \quad (16)$$

(Combined convection correlation)

The prediction by correlations is compared with the experimental result and the prediction agrees well with the experimental data. The average deviation for these two equations were about 7%. These results are valid for air and in the range of P/H = 0.1 to 0.49, 2300≤Re≤40 000, 1300000≤Ra≤13000000, and 0.4≤Ri≤ 3.

CONCLUSIONS

An experimental investigation was carried out to measure the Nu and thermal resistance of the heat sink plate under combined convection. The change in fin spacing has a different Nu which leads to heat transfer behavior prediction in the rectangular channel in various industrial applications. The following are the main conclusions of this research:

1) The combined convection heat transfer changes as the fin number changes, and maximum heat transfer takes place in the combined convection mode.
2) From the experimental results, it can be found that as the fin number increases, the Nu increases and the best result can be achieved for heat sink E by a 25% increase in Nu.
3) Our results showed that thermal resistance increases with increase in fin spacing. The lowest thermal resistance is achieved for fin number type "E" with P=4.2 mm and N=10. However, thermal resistance differences for different fin types are considerable at lower fin spacing. If fins are too close together, like type F at P=2.8 mm with N = 12, boundary layers on adjoining surfaces will coalesce and heat transfer will decrease. If fins are too far apart, like type B at P =14.6 mm with N=4, the surface area becomes too small and thermal resistance decreases.
4) Two empirical equations based on the experimental results for natural and combined convection heat transfer was developed for the average Nu as a function of the number of plates, Ri, Ra, and height ratio. The average deviation for these equations was about 7%.
5) The study resulted in the successful development of generalized empirical correlations for fin heat sinks having the capability of predicting the influence of various physical, thermal, and flow parameters on the air side performance. The experimental data has provided good design insight for studying the influence of various heat sink, flow and arrangement parameters. The Nusselt number can be determined from the generalized empirical correlations developed for plate fin heat sinks.

NOMENCLATURES

A	Area of base plate (0.48 x 0.58) m^2
Ac	cross section m^2
C_p	specific heat J/kg K
D_h	hydraulic diameter (4Ac/P) mm
g	gravitational acceleration m/s^2
Gr	Grashof number ($g \beta \Delta T L^3/\nu^2$) -
h	coefficient of heat transfer W/m^2 K
H	height of the plate m
k	thermal conductivity W/m K
I	electric current amp
N	number of plates -
Nu	Nusselt number -
P	pitch mm
Pr	Prandtl number (ν/α) -
q	supplied heat W
q"	heat flux W/m^2
Ra	Rayleigh number ($g \beta \Delta T L^3/\alpha \nu$) -
Re	Reynolds number ($\rho U D_h$)/ μ) -
T	temperature K
R	thermal resistance ($\Delta T/q$) K/W
Ri	Richardson number (Gr/Re^2) -
U	air velocity m/s
V	Voltage V

Greek symbols

α	thermal diffusivity m^2/s
β	volumetric thermal expansion 1/K
μ	dynamic viscosity N/m^2s
ρ	density kg/m^3
ν	kinematic viscosity m^2/s

Subscripts

a	ambient
av	average
b	base plate
exp	experimental
f	fluid (air)
F	force
N	natural
∞	ambient

AUTHORSHIP CONTRIBUTIONS

Authors equally contributed to this work.

DATA AVAILABILITY STATEMENT

The authors confirm that the data that supports the findings of this study are available within the article. Raw data that support the finding of this study are available from the corresponding author, upon reasonable request.

CONFLICT OF INTEREST

The author declared no potential conflicts of interest with respect to the research, authorship, and/or publication of this article.

ETHICS

There are no ethical issues with the publication of this manuscript.

REFERENCES

[1] Pourpasha H, Heris SZ, Mohammadpourfard M. The effect of TiO2 doped multi-walled carbon nanotubes synthesis on the thermophysical and heat transfer properties of transformer oil: A comprehensive experimental study. Case Stud Ther Eng 2023;41:102607. [CrossRef]

[2] Kargaran M, Goshayeshi HR, Pourpasha H, Chaer I, Heris SZ. An extensive review on the latest developments of using oscillating heat pipe on cooling of photovoltaic thermal system. Ther Sci Eng Prog 2022;1:101489. [CrossRef]

[3] Emamifar A, Moghadasi H, Noroozi MJ, Saffari H. Transient analysis of convective-radiative heat transfer through porous fins with temperature-dependent thermal conductivity and internal heat generation. J Therm Eng 2021;8:656-666. [CrossRef]

[4] Krishnayatra G, Tokas S, Kumar R, Zunaid M. Parametric study of natural convection showing effects of geometry, number and orientation of fins on a finned tube system: A numerical approach. J Therm Eng 2021;8:268−285. [CrossRef]

[5] Zolfalizadeh M, Zeinali Heris S, Pourpasha H, Mohammadpourfard M, Meyer JP. Experimental Investigation of the Effect of Graphene/Water Nanofluid on the Heat Transfer of a Shell-and-Tube Heat Exchanger. Int J Energy Res 2023;2023:3477673. [CrossRef]

[6] Barai R, Kumar D, Wankhade A. Heat transfer performance of nanofluids in heat exchanger: a review. J Therm Eng 2021;9:86−106. [CrossRef]

[7] Kobus CJ, Oshio T. An experimental and theoretical investigation into the thermal performance characteristics of a staggered vertical pin fin array heat sink with assisting mixed convection in external and in-duct flow configurations. Exp Heat Transf 2006;19:129−148. [CrossRef]

[8] Kobus CJ, Oshio T. Development of a theoretical model for predicting the thermal performance characteristics of a vertical pin-fin array heat sink under combined forced and natural convection with impinging flow. Int J Heat Mass Transf 2005;48:1053−1063. [CrossRef]

[9] Haghighi SS, Goshayeshi HR, Safaei MR. Natural convection heat transfer enhancement in new designs of plate-fin based heat sinks. Int J Heat Mass Transf 2018;125:640−647. [CrossRef]

[10] Yang MH, Yeh RH, Hwang JJ. Mixed convective cooling of a fin in a channel. Int J Heat Mass Transf 2010;53:760−771. [CrossRef]

[11] Li HY, Chao SM. Measurement of performance of plate-fin heat sinks with cross flow cooling. Int J Heat Mass Trans 2009;52:2949−2955. [CrossRef]

[12] Wang Y, Liu Y, Wang X, Zhao Q, Ke Z. Experimental study on the heat transfer and resistance characteristics of pin-fin tube. Therm Sci 2021;25:59−72. [CrossRef]

[13] Yeom T, Simon T, Zhang M, Yu Y, Cui T. Active heat sink with piezoelectric translational agitators, piezoelectric synthetic jets, and micro pin fin arrays. Exp Therm Fluid Sci 2018;99:190−199. [CrossRef]

[14] Xu Y, Gong L, Li Y, Bai Z, Xu M. Thermal performance and mechanics characteristic for double layer microchannel heat sink. J Therm Sci 2019;28:271−282. [CrossRef]

[15] Balasubramanian KR, Krishnan RA, Suresh S. Spatial orientation effects on flow boiling performances in open microchannels heat sink configuration under a wide range of mass fluxes. Exp Therm Fluid Sci 2018;99:392−406. [CrossRef]

[16] Gaikwad VP, Mohite SS. Performance analysis of microchannel heat sink with flow disrupting pins. J Therm Eng 2022;8:402−425. [CrossRef]

[17] Gandikota V, Jones GF, Fleischer AS. Thermal performance of a carbon fiber composite material heat sink in an FC-72 thermosyphon. Exp Therm Fluid Sci 2010;34:554−561. [CrossRef]

[18] Muhammed MA, Al-Hamadani AA. Study of the performance of multiple v-type fin arrangements as an enhancement of natural heat transfer from a vertical surface. J Phys Conf Ser 2021;1773:012015. [CrossRef]

[19] Ma CF, Gan YP, Tian YQ, Lei DH. Fundamental research on convective heat transfer in electronic cooling technology. J Therm Sci 1992;1:30−40. [CrossRef]

[20] Wu W, Soliman H. Performance analysis and optimization of rectangular fin arrays used in plate-fin heat exchangers. Therm Sci 2021;25:3479−3491. [CrossRef]

[21] Shim M, Ha MY, Min JK. A numerical study of the mixed convection around slanted-pin fins on a hot plate in vertical and inclined channels. Int Comm Heat Mass Transf 2020;118:104878. [CrossRef]
[22] Mohammed AA, Razuqi SA. Performance of rectangular pin-fin heat sink subject to an impinging air flow. J Therm Eng 2021;7:666−676. [CrossRef]
[23] Mohammed AA, Razuqi SA. Effect of air fan position on heat transfer performance of elliptical pin fin heat sink subjected to impinging air flow. J Therm Eng 2021;7:1406−1416. [CrossRef]
[24] Xu Y, Gong L, Li Y, Bai Z, Xu M. Thermal performance and mechanics characteristic for double layer microchannel heat sink. J Therm Sci 2019;28:271−282. [CrossRef]
[25] Rebay M, Arfaoui A, Padet J, Ben Maad R. Experimental study of the effects of a transversal airflow deflector in electronics air-cooling. J Therm Sci 2011;20:76−81. [CrossRef]
[26] El-Sayed SA, Mohamed SM, Abdel-latif AA, Abdelhamid EA. Experimental study of heat transfer and fluid flow in longitudinal rectangular-fin array located in different orientations in fluid flow. Exp Therm Fluid Sci 2004;29:113−128. [CrossRef]
[27] Wani SA, Shrotri AP, Dandekar AR. Experimental Investigation of Natural Convection Heat Transfer from a Fin Array-A Review. Int J Mod Stud Mech Eng 2016;2:46−50.
[28] Ji C, Qin Z, Low Z, Dubey S, Choo FH, Duan F. Non-uniform heat transfer suppression to enhance PCM melting by angled fins. Appl Therm Eng 2018;129:269−279. [CrossRef]
[29] El-Hakim N, Assaf J, Nehme B, Zeghondy B, Said W, Jelwan J. CFD analysis andheat transfer characteristics of printed circuit heat exchanger. J Therm Eng 2021;8:335−348. [CrossRef]
[30] Huang Y, Shen S, Li H, Gu Y. Numerical analysis on the thermal performances of different types of fin heat sink for high-power led lamp cooling. Therm Sci 2019;23:625−636.
[31] Feng S, Li F, Zhang F, Lu TJ. Natural convection in metal foam heat sinks with open slots. Exp Therm Fluid Sci 2018;91:354−362. [CrossRef]
[32] Nemati M, Sefid M. Using active/passive methods to control of MHD conjugate heat transfer of power-law fluids: a numerical entropy analysis by LBM. Int J Energy Environ Eng 2022;14:1−23. [CrossRef]
[33] Ming Z, Zhongliang L, Guoyuan M, Shuiyuan C. The experimental study on flat plate heat pipe of magnetic working fluid. Exp Therm Fluid Sci 2009;33:1100−1105. [CrossRef]
[34] Soodmand AM, Nejatbakhsh S, Pourpasha H, Aghdasinia H, Heris SZ. Simulation of melting and solidification process of polyethylene glycol 1500 as a PCM in rectangular, triangular, and cylindrical enclosures. Alex Eng J 2022;61:8431−8456. [CrossRef]
[35] Yoon Y, Kim DR, Lee KS. Cooling performance and space efficiency improvement based on heat sink arrangement for power conversion electronics. Appl Therm Eng 2020;164:114458. [CrossRef]
[36] Li HY, Tsai GL, Chao SM,Yen YF. Measurement of thermal and hydraulic performance of a plate-fin heat sink with a shield. Exp Therm Fluid Sci 2012;42:71−78. [CrossRef]
[37] Singh P, Patil AK. Experimental investigation of heat transfer enhancement through embossed fin heat sink under natural convection. Exp Therm Fluid Sci 2015;61:24−33. [CrossRef]
[38] Mithun CN, Hasan MJ, Azad AK, Hossain R, Rahman MM. Effect of unsteady relative thermal and concentration boundary layer thickness on mixed convection in a partially heated contaminated enclosure. S Afr J Chem Eng 2022;42:201−215. [CrossRef]
[39] Bergman TL, Lavine AS, Incropera FP, DeWitt DP. Introduction to heat transfer.7th ed. Hoboken: John Wiley & Sons; 2011
[40] Alizadeh H, Pourpasha H, Heris SZ, Estellé P. Experimental investigation on thermal performance of covalently functionalized hydroxylated and non-covalently functionalized multi-walled carbon nanotubes/transformer oil nanofluid. Case Stud Therm Eng 2022;31:101713. [CrossRef]
[41] Holman JP. First Order Systems. Experimental Methods for Engineers.7th ed. New York: McGraw-Hill; 2005. p.19−23.
[42] Dou HS, Jiang G, Zhang L. A numerical study of natural convection heat transfer in fin ribbed radiator. Math Probl Eng 2015;2015:989260. [CrossRef]
[43] Ayli E, Bayer O, Aradag S. Experimental investigation and CFD analysis of rectangular profile FINS in a square channel for forced convection regimes. Int J Therm Sci 2016;109:279−290. [CrossRef]
[44] Harris DC. Nonlinear least-squares curve fitting with Microsoft Excel Solver. J Chem Educ 1998;75:119−121. [CrossRef]